A MORPHOLOGICAL STUDY OF PLASMA AND PHAGOSOME MEMBRANES DURING ENDOCYTOSIS IN *ACANTHAMOEBA*

BLAIR BOWERS

From the Laboratory of Cell Biology, National Heart, Lung, and Blood Institute, National Institutes of Health, Bethesda, Maryland 20205

ABSTRACT

Particle ingestion by *Acanthamoeba* is rapid. Within 40 s bound particles can be surrounded by pseudopods, brought into the cytoplasm, and released as phagosomes into the cytoplasmic stream. In electron micrographs the phagosome appears as a flasklike invagination of the surface. Separation from the surface occurs by fragmentation of the attenuated "neck" of the invagination. The separated phagosome membrane has a three- to fourfold greater density of intramembrane particles than the plasma membrane from which it derives. This change is evident within 15 min of ingestion and is detectable while the membrane is still tightly apposed to the particle. There is no direct evidence for the mechanism of this increase; no increase in particle density was seen in the membrane at an early stage in the forming phagosomes still connected to the surface. These morphological observations are consistent with chemical analyses, to be reported in a separate communication, that show that the phagosome membrane has a higher protein to phospholipid ratio and a higher glycosphingolipid content than the plasma membrane. Enlarged phagosomes (presumptive phagolysosomes) show multiple small vesiculations of characteristic morphology. The small vesicles are postulated to be the major route of membrane return to the cell surface.

KEY WORDS *Acanthamoeba* · phagocytosis · membrane structure · freeze-fracture replication

It has been recognized for several years, from a variety of studies on endocytosis and cell secretion, that the membrane of the cell surface may cycle through the cytoplasm (e.g., references 12, 20, 21, and 28). The cellular mechanisms involved in membrane recirculation are not yet understood, and in fact may differ in different cell types. Endocytosis in protozoa is a useful experimental system for examination of membrane recirculation because endocytosis is the normal feeding mechanism, can be controlled experimentally, and results in a high rate of membrane use. In the ciliates, for example, there is a well-defined route of food vacuole formation and processing that is particularly accessible to morphological analysis because the vacuole forms and is discharged through specific sites on the cell surface. Although some molecular changes in the vacuolar membrane may also take place (13), the food vacuole cycle in ciliates appears to be one of the clearest examples of membrane reuse in bulk (1, 3, 4, 14, 17). In these organisms an intracellular pool of membrane is used to form the food vacuoles so that the recirculating membrane remains intracellular (1, 3). In amebas and mammalian cells, on the other hand, the mechanism is different: the surface membrane is used to form endocytic vesicles.

Quantitative studies of pinocytosis (which unlike phagocytosis is a continuous process) in *Acanthamoeba* (7), macrophages, and L cells (24) suggest that these cells ingest and recirculate a quantity of membrane equivalent to the entire cell surface in a period of minutes. The route of membrane passage appears to include the vacuolar-lysosomal system of these cells (24), but it is not known whether there is mixing of surface and lysosomal membrane components after fusion or what mechanisms serve to return membrane to the cell surface.

In this and other studies to be reported, we have used *Acanthamoeba castellanii* as an experimental system to investigate interrelationships of membranes involved in the endocytic pathway. In the present study we have examined phagocytosis in *Acanthamoeba* by time-lapse movies, thin-section and scanning electron microscopy, and freeze-fracture replication.

The investigation gives new information about the timing and mode of phagosome formation. It shows that the membrane of the phagosome is structurally different from the plasma membrane when observed in freeze-fracture replicas, suggesting compositional changes during or after internalization. Several possibilities for the mechanism of the structural changes were examined. These and other observations to be presented suggest that a major portion of membrane returns to the surface via small vesicles, but that the mechanism may be more complex than a simple reinsertion of unaltered plasma membrane by way of small vesicles or defecation vacuoles deriving from the phagosome.

MATERIALS AND METHODS

Acanthamoeba castellanii (Neff strain) was cultured as described previously (5). For phagocytosis studies, lipid-extracted baker's yeast suspended in 0.1 M sodium phosphate buffer, pH 6.8, was added to *Acanthamoeba* cells in culture medium at 30°C on a reciprocating shaker.

To fix cells for freeze-fracture replication, glutaraldehyde in 0.1 M sodium phosphate buffer, pH 6.8, was added to the cell suspension to a final concentration of 1.5%. The cells were fixed for 30 min at 30°C and rinsed briefly in 0.1 M phosphate buffer before being carried through increasing concentrations of glycerol in the same buffer. The cells were frozen in 30% (wt/vol) glycerol in liquid nitrogen cooled to its freezing point by evaporation under vacuum or in liquid nitrogen-cooled Freon 22. Replicas were made on a Balzers 360 M (Balzers Corp., Nashua, N. H.) using a complementary replica device for fracturing and an electron beam evaporation unit for platinum shadowing.

The intramembrane particle density of plasma membrane fracture faces was assessed in micrographs printed at × 114,000. "Windows" equivalent to 0.25 or 0.0625 μm^2 were dropped on areas of the fracture faces with minimal tilt, and all the particles showing within the window were counted. For estimation of intramembrane particle size, shadow widths were measured to the nearest 0.5 nm at 90° to the shadow direction using a dissecting microscope with a micrometer eyepiece at a total magnification of 1.4×10^6. All of the particles within a window were measured, and two to four windows per fracture face were counted until a total area of 1 μm^2 was accumulated.

The structure of the plasma membrane of *Acanthamoeba* was examined after freezing unfixed cells removed directly from culture medium and after prefixing in glutaraldehyde and glycerinating. No significant differences in membrane structure were observed. Fixation, followed by glycerination, was routinely used in this study to avoid ice crystal damage of intracytoplasmic structures.

Time-lapse photographs were made of cells in a Dvorak-Stotler culture chamber (Nicholson Precision Instruments, Bethesda, Md.) at a speed of five frames per second.

For thin sections, cells were fixed for 1 h at room temperature in 3% glutaraldehyde in 0.1 M sodium phosphate buffer, pH 6.8, postfixed in 1% osmium tetroxide for 1 h, dehydrated in ethanol, and embedded in Epon 812. For tracer studies, 1 mg/ml horseradish peroxidase (Sigma Chemical Co., St. Louis, Mo.) was added to the culture medium, and glutaraldehyde-fixed cells were incubated in diaminobenzidine according to Graham and Karnovsky (11) before postfixation in osmium tetroxide.

Scanning electron microscopy was performed on *Acanthamoeba* fixed in suspension with 3% glutaraldehyde in 0.1 M phosphate buffer, pH 6.8. Cells were dehydrated in ethanol and critical point dried from CO_2. The dried cells were coated with carbon and gold-palladium before scanning on a Jeol JSM-35 electron microscope.

RESULTS

Temporal Aspects of Phagocytosis

Time-lapse movies show that contact and binding of a particle do not necessarily result in ingestion. Amebas were observed to crawl over or under particles (yeast or latex beads) or drag bound particles along with them for some time without ingestion. In one case, food cup formation was observed adjacent to an adhering but nonphagocytosed particle. Scanning electron microscope images show clearly that the acanthopods bind particles and therefore probably play an important role in particle capture by increasing the effective volume for particle capture. Both the movies and SEM observations show no preferential uptake by particular regions of the surface (e.g., the uropod). When the "decision" is made by the ameba to ingest, engulfment takes place rapidly and is carried to completion.

Eight ingestion sequences were studied by time-lapse cinematography. Two events that could be identified precisely at the light microscope level were the initial contact of the yeast with the cell and the moment at which the ingested yeast

showed motion in the cytoplasmic stream within the cell. In one sequence, a cell was observed to drag a particle around for some minutes, undergo cell division, and then ingest the particle over the next 63 s. The minimum time observed between the first contact between the ameba and the particle and the appearance of the particle in the cytoplasmic stream was 35 s. In one other case, where the orientation of the particle was favorable, it was estimated that the closure of the pseudopods around the particle took ~26 s and the entrance of the particle into the cytoplasmic stream an additional 13 s.

Morphology of Phagocytosis

To relate the replica image to the more familiar thin-section image, low magnification views of *Acanthamoeba* that have ingested yeast are shown in Figs. 1 and 2. After short periods of incubation with particles, the cells contain both "empty" vacuoles, whose history is unknown, and newly formed phagosomes with yeast. The bulk of the membrane surrounding an ingested particle is derived directly from the plasma membrane, and, as shown in Fig. 3, is added to by fusions with pinosomes which also are derived from the plasma membrane. Phagosomes rapidly acquire hydrolytic enzymes (22, 29) by an as yet unidentified route, but presumably by fusion with enzyme-carrying vesicles. Such vesicles, if they add to the membrane of the phagosome, are the only likely source of phagosome membrane not directly derived from the plasma membrane.

Both time-lapse movies and scanning electron microscope images suggest that the cell flows out around the particle to be ingested. Possibly, as a consequence of the rapid entry process, relatively few images of the stages between binding and the presence of the particle in the separated phagosome were observed in replicas or thin sections. Freeze-fracture replicas show more clearly than thin sections the way in which the phagosome forms (Figs. 4 and 5). Fig. 4 illustrates a slightly earlier stage than Fig. 5, which shows the development of the tubular connection of the phagosome to the surface. The opening of the tubular surface connection can be distinguished in scanning electron micrographs (Fig. 6). In this instance the opening is 0.8 μm in diameter and corresponds to a stage in which the opening is slightly more constricted than in Fig. 4. The final separation of the phagosome appears to occur by elongation and eventual closure of the attennuated neck (Figs. 7 and 8). The fusion event therefore involves only a small area of membrane and is the same regardless of the size of the particle ingested.

In the formation stage of the phagosome the invaginated surface membrane is surrounded by a microfilamentous complex, previously illustrated in thin section (16). Freeze-fracture replicas (Figs. 4 and 5) do not resolve individual filaments, but clearly show the exclusion of other cell organelles from the vicinity of the invaginated membrane. Thin sections indicate that only glycogen particles infiltrate the filament network, and these can also be seen in the replicas. The remnant of the phagosome neck remains embedded in the microfilamentous complex after the filaments are no longer associated with the phagosome itself (Fig. 7).

Plasma Membrane Morphology

The structure of *Acanthamoeba* plasma membrane as seen in freeze-fracture replicas is shown in Fig. 9 *a* and *b*. The protoplasmic face (PF) has about twice the intramembrane particle (IMP) density as the extracellular face (EF), and the particles of the PF are more distinct (i.e., extend farther above the fracture plane) than those of the EF. Both fracture faces contain elongate elements that are more difficult to visualize than the round particles. The elongate particles appear to be integral parts of the membrane (as opposed to an indentation produced by cytoplasmic elements lying apposed to the other side of the bilayer)

FIGURE 1 Thin section of a cell allowed to phagocytize yeast. Two yeast particles (*Y*) have been ingested and one is bound to the surface by acanthopods outside the plane of section. Arrow points to cross section of an acanthopod. Cell contains a number of large digestive vacuoles (*V*), which are functionally equivalent to phagosomes. *N*, nucleus. × 7,400. Bars are 1 μm, except in Figs. 9–14 and 17, where bars are 0.1 μm.

FIGURE 2 Freeze-fracture replica of cell exposed to yeast 60 min. Cell boundary is indicated by arrows. Two phagosomes show clear evidence of yeast contained within them (asterisks). *N*, nucleus; *G*, Golgi apparatus. × 7,400.

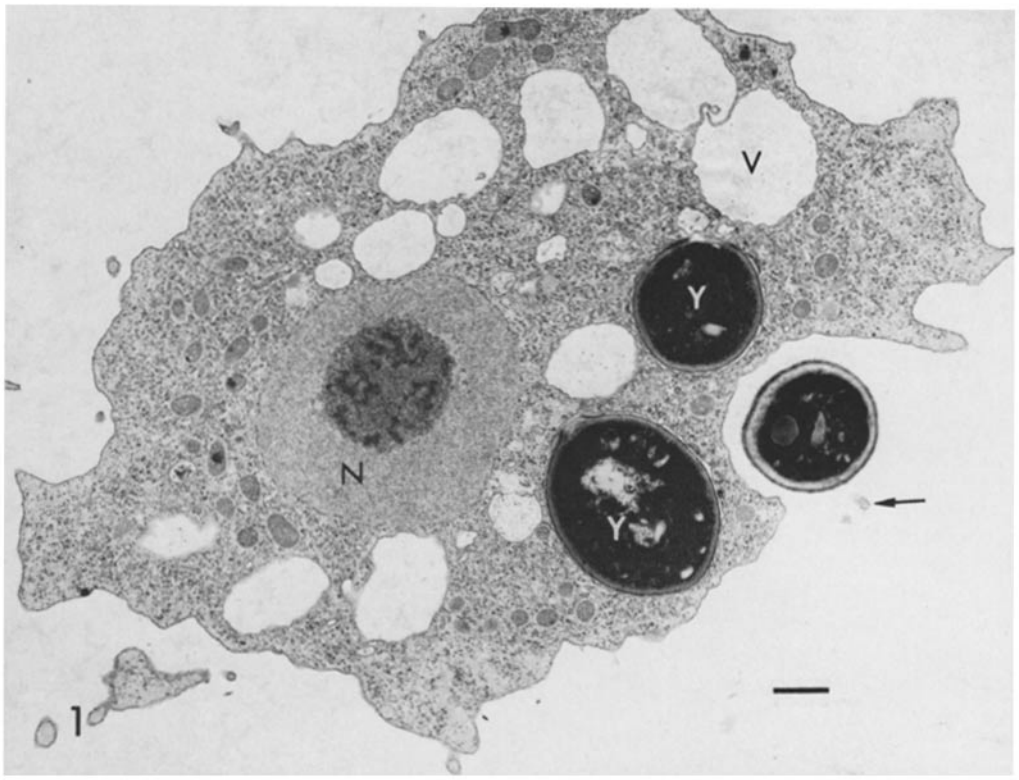
V
Y
N
Y
1

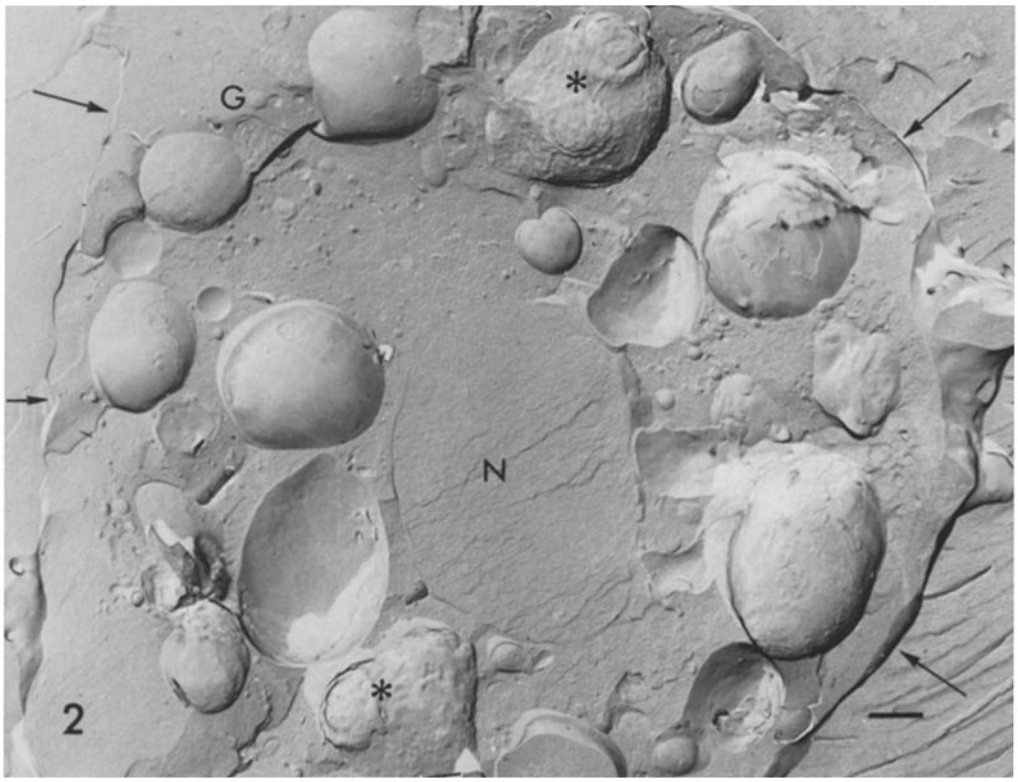
G
*
N
*
2

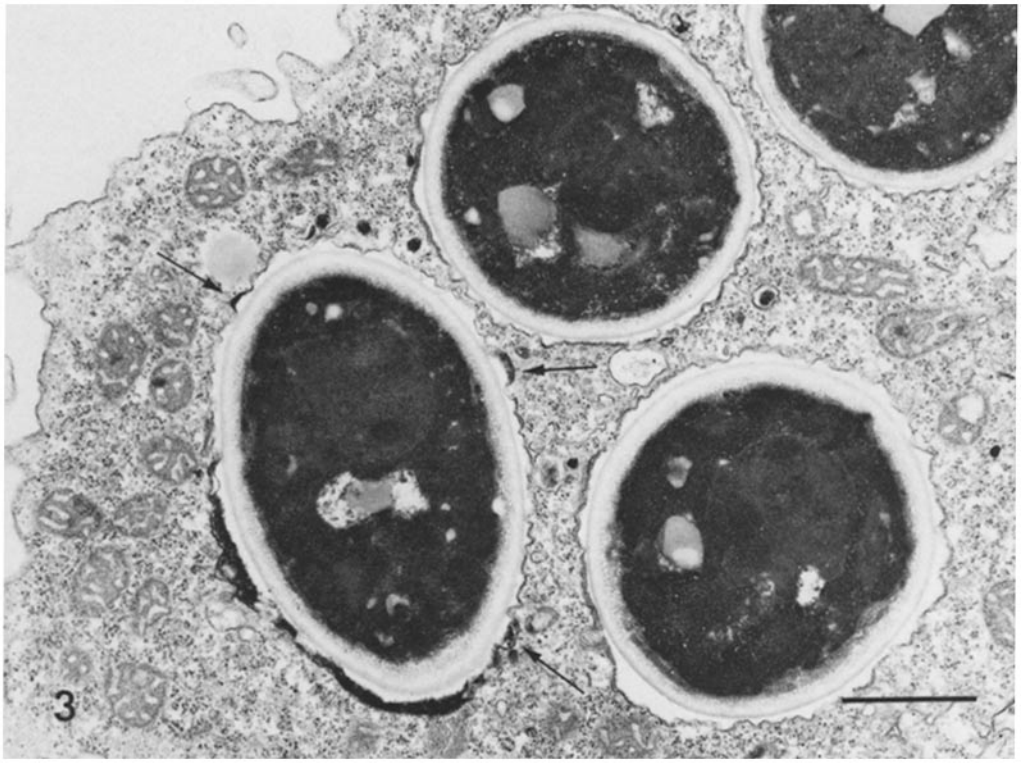

FIGURE 3 Cells were incubated in medium containing yeast and 1 mg/ml horseradish peroxidase (HRP) for 30 min before fixation. A number of small pinocytic vesicles (pinosomes) labeled with HRP are seen in the cytoplasm. Arrows point to sites of fusion of labeled pinosomes with one of the phagosomes. × 17,900.

because they are translocated with the other IMP when the membrane undergoes phase separation (Fig. 12). In addition, the PF is characterized by a class of small IMP, ~7.5 nm in diameter, that often show a specific association with each other as contiguous clusters of three to five particles (8, 23). The measured particle density on any given face varies because of differences in replication technique (e.g., shadow angle and replica thickness) and because IMP are not uniformly distributed and may vary in number on account of the physiological state of the cell. The IMP density on the EF is in the range of 100–200 particles/μm^2 and on the PF, 200–400 particles/μm^2.

Phagosome Membrane Morphology

The fracture faces of large vacuoles in nonphagocytosing cells have a higher density of IMP than plasma membrane faces. Empty vacuoles are normally present in the cell (6), but they disappear as the cell fills with phagosomes (22). The vacuoles, which form by pinocytosis of the culture medium, contain acid hydrolases (22) and appear to be functionally similar to phagosomes, but neither the time-course of their existence nor their origin can be precisely determined. On the other hand, the source of most of the membrane surrounding phagosomes and the approximate lifetime of the phagosome can be specified. For these reasons, particle densities were measured only in phagosome membranes. Phagosomes in the replica can be identified unambiguously by the unique configuration of the bud scar region of the yeast underlying the replicated membrane (Fig. 2). The fracture faces of a phagosome membrane are shown in Fig. 10 *a* and *b*. The IMP density on these faces is about fourfold greater than that found on a similar sample of plasma membrane (Figs. 9 and 11). The same asymmetry is maintained in the phagosome membrane as in the plasma membrane, that is, the EF shows about one-half the IMP density as the PF. There is also a similar

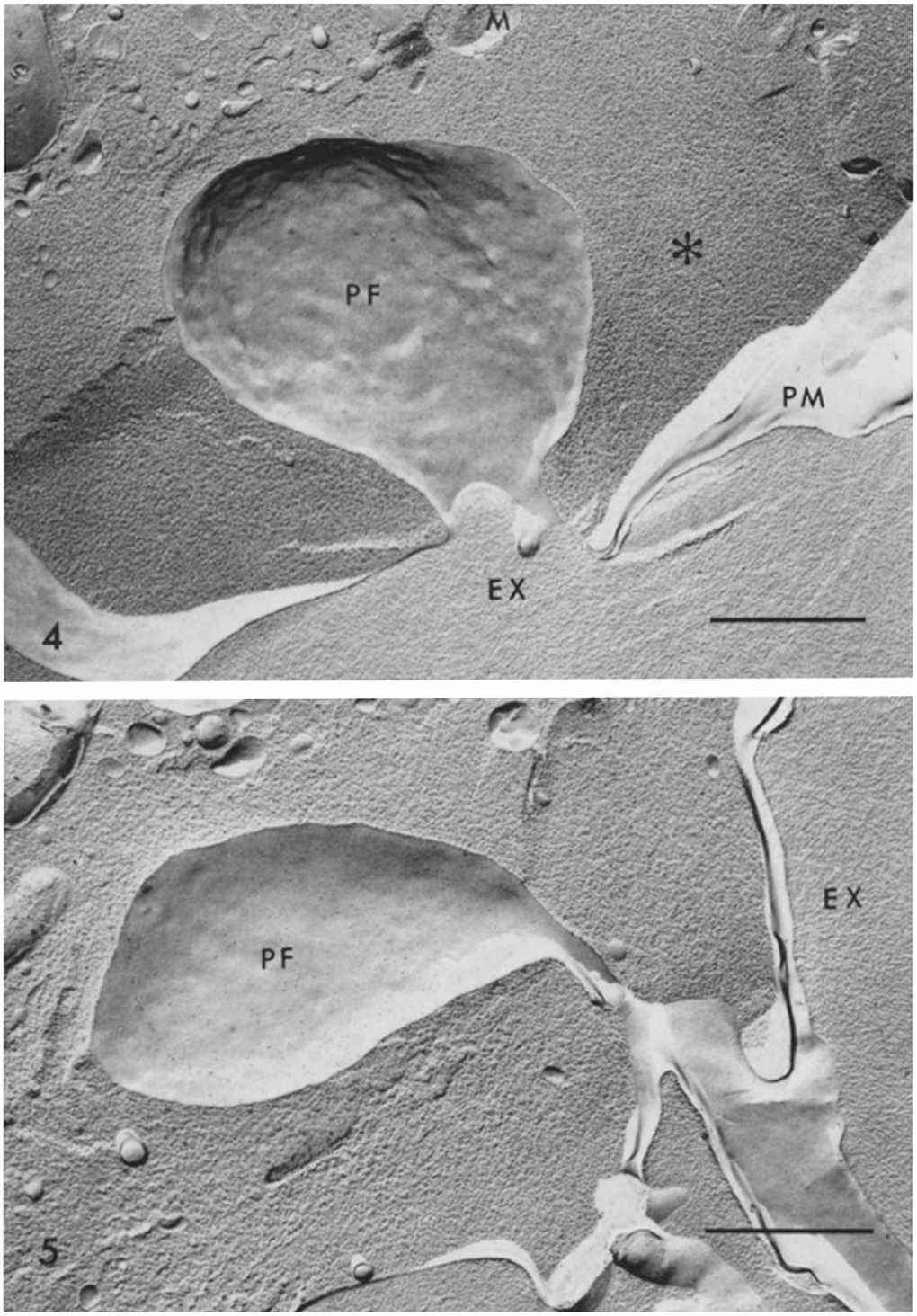

FIGURE 4 *Acanthamoeba* exposed to yeast particles for 15 min before fixation. Note that the area of cell cytoplasm (asterisk) surrounding forming phagosome is free of mitochondria and membranous elements of the cytoplasm. In thin section this area is seen to be filled with microfilaments. The pebbled appearance of cytoplasm is caused by glycogen particles which partially infiltrate the microfilamentous matrix. The apparent diameter of the phagosome neck is 0.7 μm. *EX*, extracellular space; *PF*, protoplasmic face of phagosome membrane; *M*, mitochondrion; *PM*, plasma membrane. × 22,800.

FIGURE 5 Later stage in phagosome formation. Phagosome retains a narrow, tubular connection with the cell surface, apparent diameter 0.2 μm. As in Fig. 1, larger cytoplasmic structures are excluded from the vicinity of the phagosome membrane, but the zone of exclusion is more extensive around the neck of the phagosome. × 25,100.

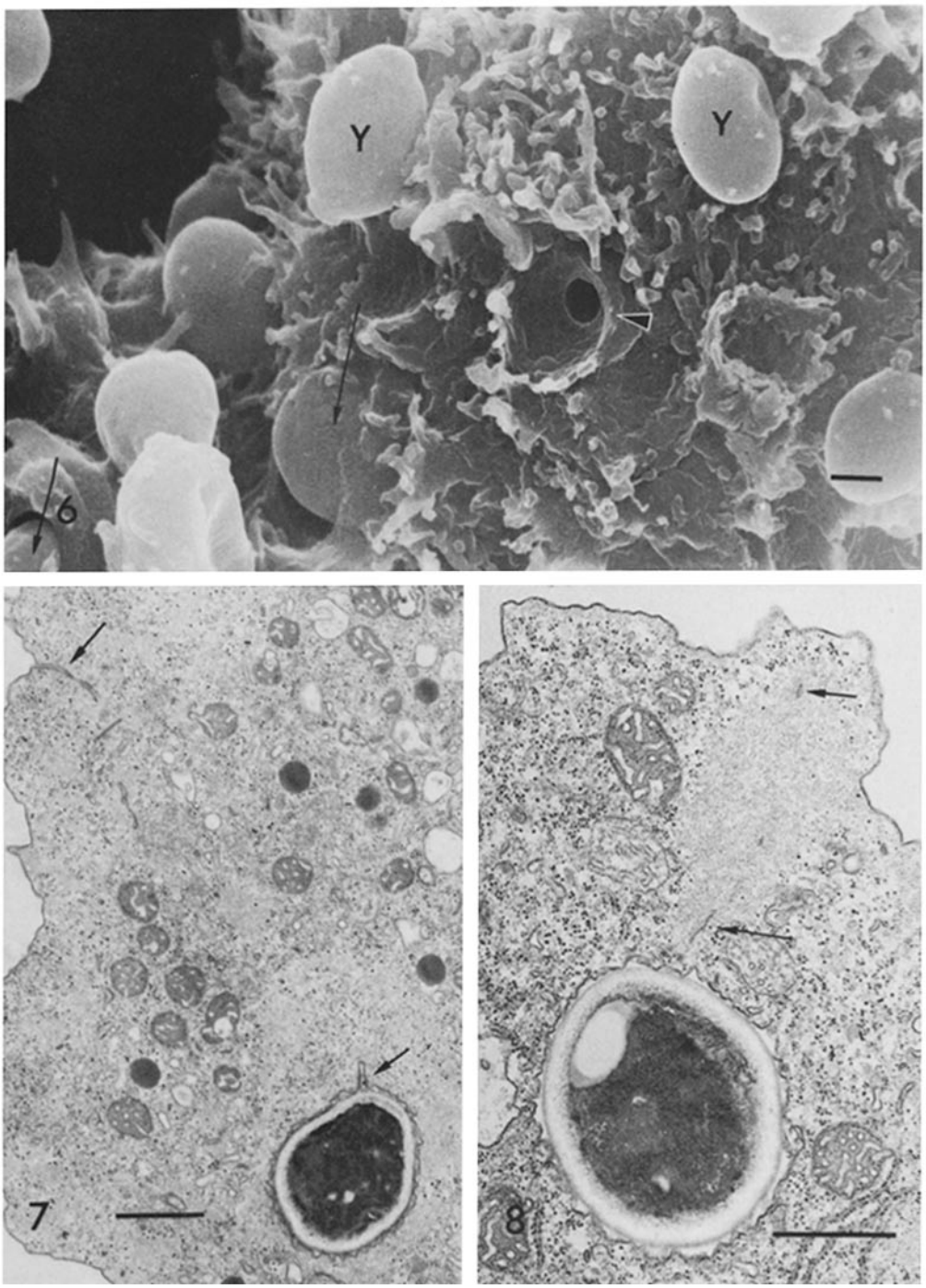

FIGURE 6 Scanning electron micrograph showing mouth of phagosome (arrowhead), ~0.8 μm in diameter. The cell surface has several bound yeast (*Y*) and shows many surface projections. Arrows indicate two yeast that appear to be in the process of ingestion. × 7,040.

FIGURE 7 Thin section of phagosome showing short portion of neck and at some distance another (or a part of the same) attached to the surface (arrows). The apparent diameter of the neck is 0.08 μm. In this instance the phagosome still retains the layer of microfilaments around it. × 13,000.

FIGURE 8 Thin section of completed phagosome showing remnants of neck (arrows) in the microfilament complex. Microfilaments no longer are present around phagosome membrane, and mitochondria and large vesicles are found close to phagosome. × 17,800.

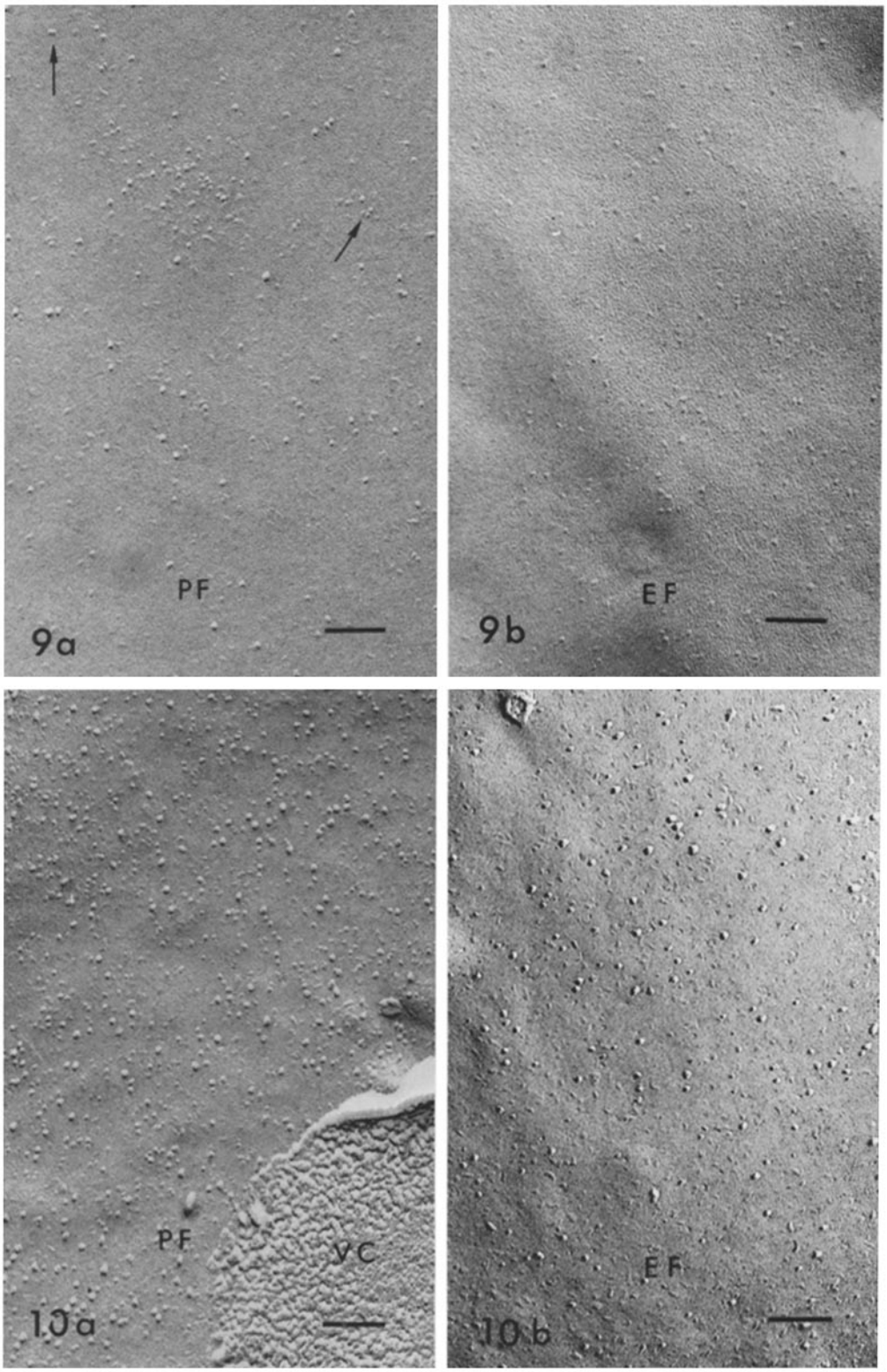

FIGURE 9 Fracture faces of *Acanthamoeba* plasma membrane. (*a*) Protoplasmic face (*PF*). Arrows show clustering of smaller particles that is characteristic of this face. (*b*) Extracellular face (*EF*). IMP are not so easily seen on this face as on PF and are about half the density. × 92,000.

FIGURE 10 Fracture faces of phagosome membrane. (*a*) Protoplasmic face (*PF*). IMP density is higher than the corresponding face of the plasma membrane. *VC*, vacuole content which contained cross-fracture of yeast. (*b*) Extracellular face (*EF*). Not only is IMP density higher than corresponding face of the PM, but the IMP are much more prominent. Density of IMP on the phagosome EF is about half that on the PF. × 92,000.

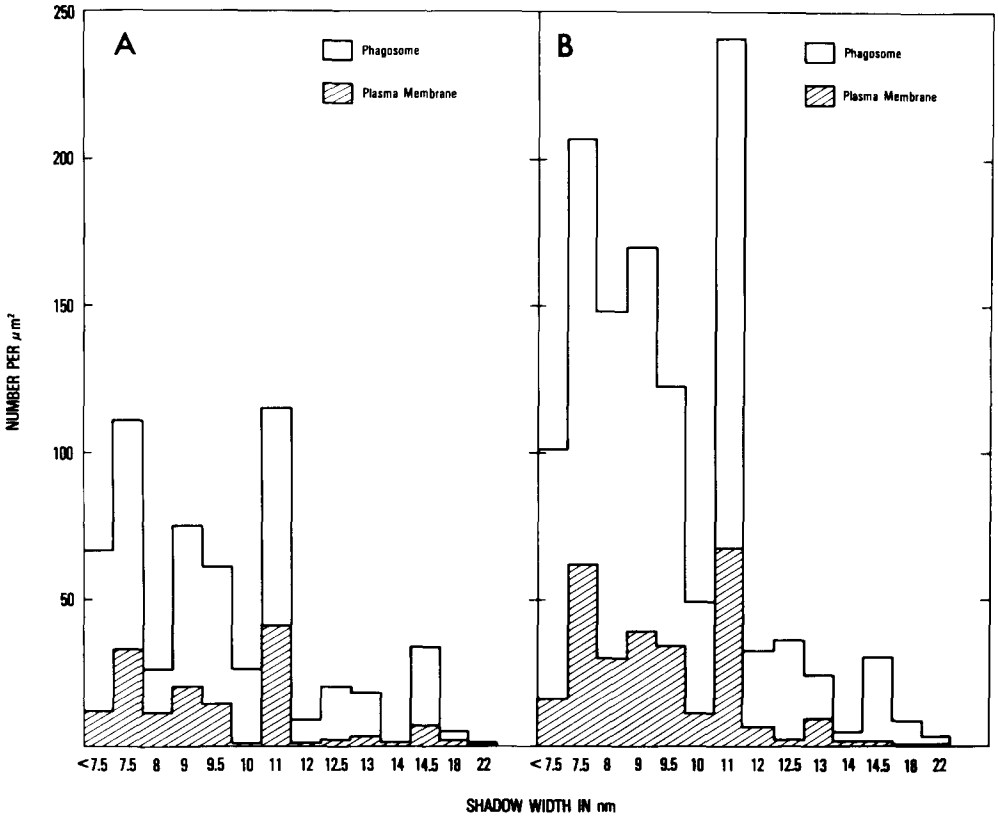

FIGURE 11 Intramembrane particle sizes on plasma membrane and phagosome membrane fracture faces. Measurements of particles were made as described in Materials and Methods. (*A*) Extracellular face. Ratio of phagosome IMP to plasma membrane IMP is 4.2. (*B*) Protoplasmic face. Ratio of phagosome IMP to plasma membrane IMP is 3.8.

distribution of size classes in both the plasma membrane and the phagosome membrane (Fig. 11). The increase in IMP density is evident at least within 15 min of ingestion, which was the shortest time examined in this study.

Two possible routes of IMP density increases in phagosomes can be readily investigated in replicas: (*a*) selective inclusion and concentration of IMP in the forming phagosome, and (*b*) fusion of cytoplasmic membranes with very high IMP content with phagosomes. Particle densities were counted at high magnification in several forming phagosome membranes similar to stages shown in Figs. 4 and 5, and no increase in IMP over that of the plasma membrane was found. There was also no indication of increased IMP number or aggregation at a site where yeast was bound to the surface but with no evidence of ingestion. Likewise, examination of vesicle associations with phagosomes (Figs. 13 and 14) gave no evidence that IMP increase occurred by fusion of membrane with high IMP content. The contractile vacuole, endoplasmic reticulum, nuclear envelope, and mitochondrial membranes all had higher IMP density than phagosomes, but there was no evidence in thin sections or in freeze-fracture replicas that these systems fuse with phagosomes.

Low magnification micrographs of replicas show large numbers of small (50-200 nm) vesicles in the cytoplasm of *Acanthamoeba*. Because pinocytosis is markedly reduced during phagocytosis (5), most of these small vesicles must have another origin. The phagosomes appear to bud off large numbers of vesicles during their life cycle in the cytoplasm, and this is particularly well shown in freeze-fracture replicas. Fig. 15 shows the extracellular face of an enlarged phagosome (identified by the impression of a yeast bud scar in the center) which probably resulted from the fusion of two or more phagosomes. The exposed fracture face has

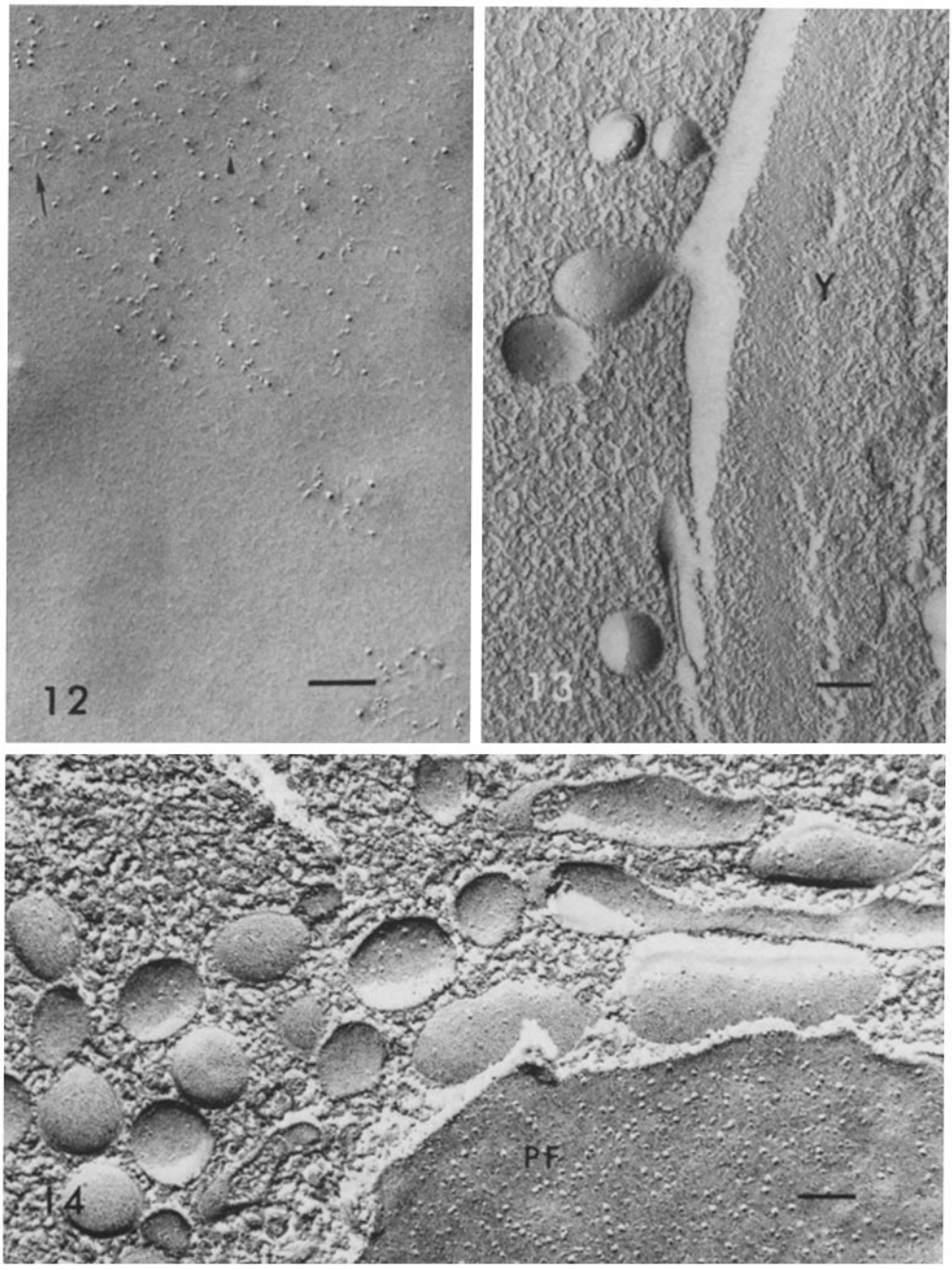

FIGURE 12 Phase separation in the plasma membrane was induced by slow cooling of unfixed cells in the presence of glycerol. The three morphologically distinct IMP are shown especially well: large particles (~11 nm), small particles (~7.5 nm) that show characteristic clusters (arrowhead), and elongate elements (long arrow) that do not show plastic deformation characteristic of the other two particle types. × 92,000.

FIGURE 13 Cross-fracture of phagosome closely enclosing a yeast cell (*Y*) with attached small vesicle. × 79,100.

FIGURE 14 Protoplasmic face of vacuole (*PF*) showing association of many small vesicles with lower IMP density. × 81,000.

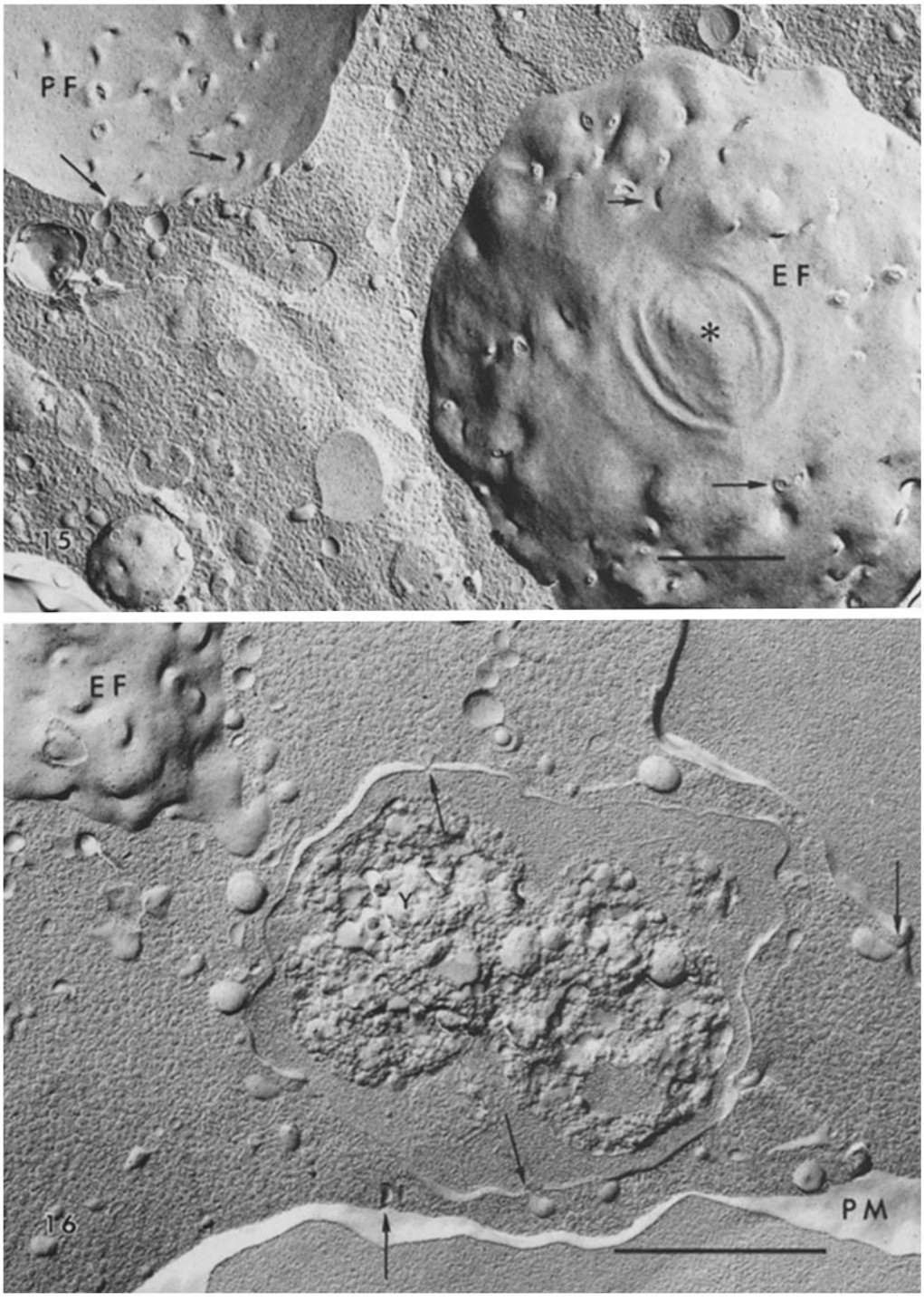

FIGURE 15 Cells exposed to yeast 120 min before fixation. One large vacuole shows evidence of yeast content (asterisk). Both vacuoles show evidence of many small vesiculations of their surfaces (arrows). The vesiculations result in a characteristic semicircular bulge on the PF and a corresponding depression on the EF. × 18,600.

FIGURE 16 Cells exposed to yeast 45 min before fixation. Cross-fractured phagosome appears to contain two partially digested yeast (*Y*) indicating that it is a late stage. Small vesicles can be seen attached to membrane (arrows). Extracellular face (*EF*) of adjacent vacuole also shows evidence of much vesiculation. Arrows at plasma membrane (*PM*) indicate vesicles that appear to be joining the PM. × 31,500.

66 vesiculation sites. In the same image is a portion of the protoplasmic face of a vacuole or phagosome membrane also with a large concentration of vesiculation sites. The fracture on the latter vacuole occurred in such a way as to show the attachment of one of the vesicles to the vacuole. In some vacuoles the vesiculation sites are confined to smaller areas of the surface, but they are always clustered. Fig. 16 shows several vesiculation sites on a cross-fractured phagosome in which the contents appear to be partially digested.

The vesicles associated with the vacuoles, and equivalent phagolysosomes, show a characteristic morphology. There is a crescent-shaped indentation toward the extracellular side of the membrane (Figs. 15 and 16). Fig. 17 illustrates the structure of the sites at higher magnification, showing the same appearance in a cross-fracture as well as in *en face* views of the split membrane. On the protoplasmic fracture face the crescent-shaped bulge shows an accumulation of large intramembrane particles, sometimes aligned in rows (Fig. 17 *d*). There is a range of sizes in the fractured necks of adjacent vesiculations (Fig. 17 *b*), suggesting that the process is only relatively synchronized. Presumably, these structural characteristics are related to the cellular mechanisms that effect the formation and separation of small protrusions from a smooth surface.

DISCUSSION

A central observation reported in this study is an alteration in membrane structure that occurs after plasma membrane is internalized as phagosome membrane. The questions that can be addressed are: what do the structural changes represent in chemical and functional terms, when do they occur, and by what mechanism? These questions also relate to routes and mechanisms of membrane recirculation in *Acanthamoeba*, as there is biochemical evidence in this ameba that there must be recirculation accompanying the high rate of continuous endocytosis (7, 15).

There is considerable evidence that proteins that extend into lipid bilayers are visible as particles in freeze-fracture replicas of the split bilayer (27). It is not known whether all intercalated proteins are visible as particles, but the density of IMP is correlated with the metabolic activity of the membrane (9), implying some proportionality between protein content and IMP density. There is, in addition, some recent evidence that certain lipid moieties may appear as IMP in freeze-fracture replicas (25, 26).

There are several possible explanations for IMP density increase, including artifact caused by contamination of the replicas. Condensation of water vapor or other gases on the specimen before replication can duplicate the appearance of IMP. It is unlikely that contamination accounts for increased IMP in this case, for the following reasons: the differences were consistently observed; closely adjacent membranous vesicles show no or few IMP; and the similarity between the pattern in the size distribution of IMP on the phagosome membrane and that of the plasma membrane would not be expected if the phagosome membrane were contaminated.

IMP density change in membrane after phagocytosis has also been reported in two ciliates. In *Paramecium*, Allen (2) reported the opposite of what we observed in *Acanthamoeba*. The circulating food vacuole has fewer total IMP per unit area than the surface from which it derives, and there is a reversal of the particle asymmetry between the fracture faces. In *Tetrahymena*, on the other hand, Kitajima and Thompson (13) find a situation similar to that observed in *Acanthamoeba*. Within 1–4 min after the food vacuole separates from the surface, there is a twofold increase in IMP density on the P face. They have further shown that the separated vacuole has a higher phase transition temperature than the forming vacuole, suggesting alteration in the physical environment of the lipids or in the lipid composition in the separated vacuole. In contrast to the three protozoan systems, no changes of IMP density were observed in phagosomes of the polymorphonuclear leucocyte (18).

The increased density of IMP in *Acanthamoeba* implies either a change in the molecular composition of the phagosome membrane or a change in the conformation or association of molecules so that the appearance of IMP is enhanced. A direct way of distinguishing between these alternatives is to measure the protein/lipid ratio in isolated phagosome membranes and compare it with similar measurements on plasma membranes. We (A. H. Chagla and B. Bowers) are currently making such an analysis, and the results indicate a higher protein to phospholipid ratio as well as increased glycosphingolipid content in the phagosome membranes as compared to plasma membranes (10). These findings, of course, do not rule out that physical state changes in addition to compositional changes may occur.

The exact time in the phagocytic sequence at

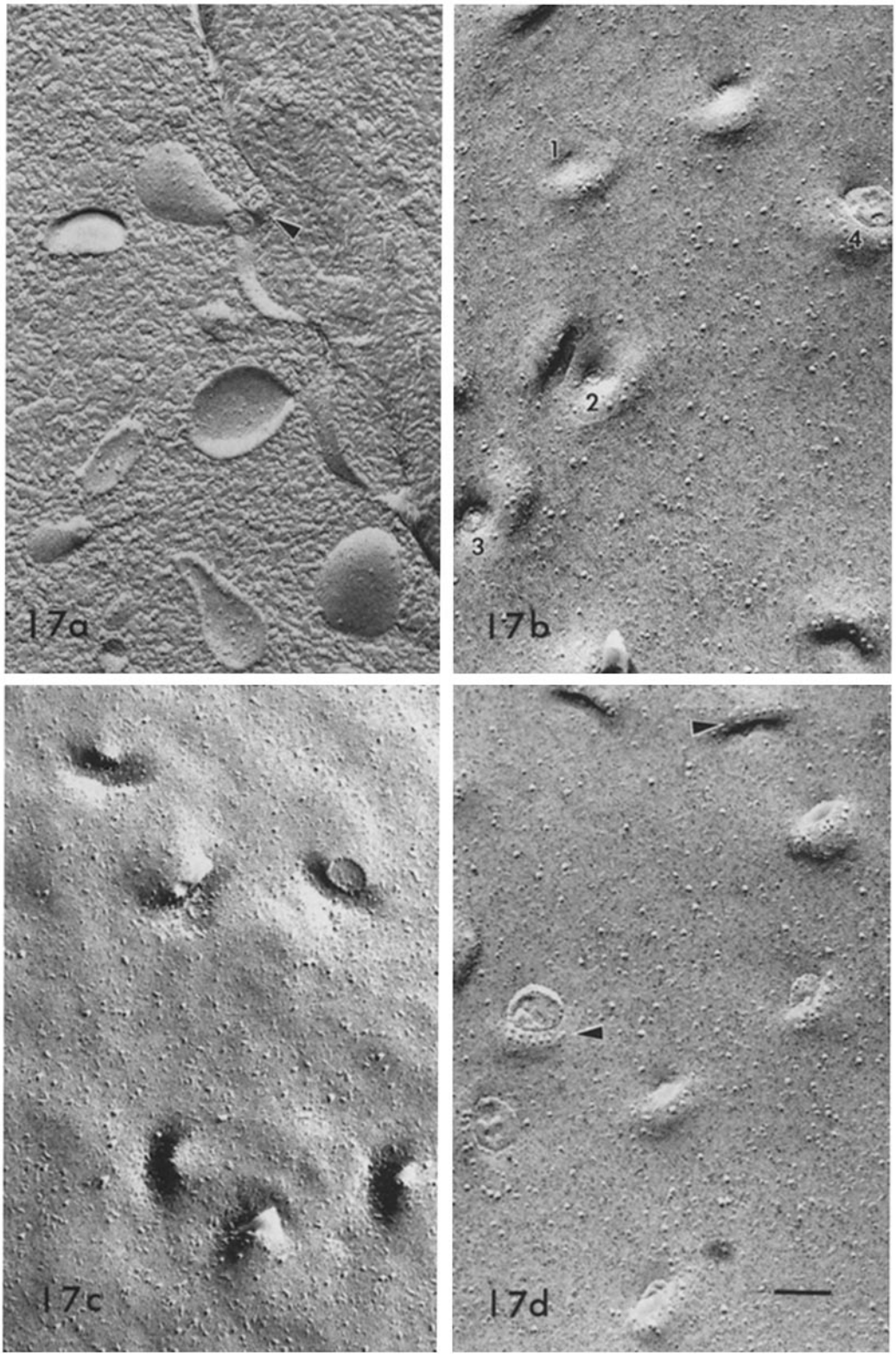

FIGURE 17 Freeze-fracture replicas showing vesicle attachments to vacuoles. (*a*) Cross fracture of vesicle attachment site in which the characteristic bulge is seen on one side (arrow). (*b*) Protoplasmic fracture face of vacuole membrane with a number of vesiculation sites in which a range of opening sizes are visible (*1–4*). (*c*) Extracellular fracture face of vacuole membrane showing vesiculation sites with structure complementary to protoplasmic face. (*d*) Protoplasmic fracture face showing large particle accumulation on crescent-shaped bulge around vesiculation sites (arrows). × 85,700.

which the structural alteration of the membrane occurs in *Acanthamoeba* has not yet been identified, but this study suggests that the change becomes detectable morphologically shortly after separation of the phagosome from the surface. The time-lapse observations document that the events of engulfment and membrane flow that form the phagosome and the final separation from the cell surface can take place within 40 s. Thus, the dispersion of the microfilamentous matrix and the fusion event that closes the connection to the cell surface are essentially simultaneous events that release the phagosome to move freely in the cytoplasmic stream. At that point the surface of the phagosome is accessible for fusions or other cytoplasmic interactions that might modify the membrane structure. Old and new phagosomes and remaining vacuoles appear to mix randomly in the cytoplasmic stream, so it is difficult to determine whether changes occur randomly as a consequence of interaction with other cytoplasmic components or whether they occur after some precise sojourn in the cytoplasm. The present data indicate only that changes can take place within 15 min of ingestion.

There are a number of possible mechanisms for alteration of the structure of the phagosome membrane, and the present study identifies likely ones for further investigation. There is no morphological evidence for insertion of protein by fusion with vesicles with very high IMP density, although other routes of protein addition are not ruled out. The increase is not a function of the presence of the yeast itself in the vacuole, as increased IMP density also was observed in vacuoles of cells that had not ingested yeast. The freeze-fracture replicas document a very large flux of small vesicles in the cytoplasm of *Acanthamoeba*. Most of these vesicles are too small and have a radius of curvature too great to permit accurate measurement of their IMP density, but some larger ones clearly have few or no IMP. Thus, a possible mechanism is one of concentration of protein and glycosphingolipid in the phagosome membrane by budding off small vesicles that are predominantly phospholipid. This mechanism seems unlikely, however, because the changes in IMP were observed in phagosomes in which the membrane still appeared to tightly surround the phagocytosed particle. It is clear from the topography of the forming phagosome—a flask-shaped pouch, ultimately closely following the contours of the ingested object—that considerable molecular rearrangement (flow) of the lipid bilayer must take place during the process. Most of the flow must occur while the bilayer is closely associated with (presumably connected to) the matrix of microfilaments that is seen to underlie the membrane at this time. Given the morphological description of phagocytosis presented here, a working hypothesis is that some proteins may be immobilized by their association with the microfilaments on the cytoplasmic side of the membrane (19) and that the glycosphingolipid may be relatively immobilized by an association at the extracellular surface with the particle being ingested. As a consequence, both may be enriched in the membrane while the phospholipid is free to flow back into the surface. In the early stages of phagosome formation observed in freeze-fracture replicas (Figs. 4 and 5), there were no detectable changes in the density or distribution of the IMP, so that if such a mechanism pertains, the IMP density increase may manifest itself only in later stages of the phagosome formation or perhaps in conjunction with changes in the pH or ionic content of the phagosome after separation from the surface.

From the static images of electron microscopy, it is not possible to state unequivocally that the many small vesicles seen attached to vacuoles are budding off rather than fusing; however, budding is the most plausible interpretation. Phagosomes fuse with each other and reduce the mass of the contained material by digestion. The excess vacuolar membrane is in some way removed, and it is removed by a process that results in recirculation of most of the membrane. The attached vesicles are particularly numerous on enlarged vacuoles of the type which are likely to be reducing their surface area (Figs. 16 and 17). We also know that pinocytic vesicles, which are similar in size and the major source of fusing vesicles (Fig. 3), are markedly decreased in number during phagocytosis (5). The semicircular bulge in the plane of the vacuolar membrane presumably is related to cytoplasmic events that bring about the vesiculations. The accumulation of IMP on the bulge may reflect specific associations of membrane proteins with cytoplasmic elements, but the cytoplasmic structure is not sufficiently well defined by the standard thin-sectioning techniques used in this study to discern what they might be.

This study benefited from the skilled assistance of Thomas E. Olszewski with the freeze-fracture replicas and of Margaret L. Clark with photographic printing. I

thank Dr. Emma Shelton for use of the scanning electron microscope, and Drs. E. D. Korn and C. F. Bailey for critical readings of the manuscript.

Received for publication 10 September 1979.

REFERENCES

1. ALLEN, R. D. 1974. Food vacuole membrane growth with microtubule associated membrane transport in *Paramecium*. *J. Cell Biol.* **63**:904–922.
2. ALLEN, R. D. 1976. Freeze-fracture evidence for intramembrane changes accompanying membrane recycling in *Paramecium*. *Cytobiologie.* **12**:254–273.
3. ALLEN, R. D., and R. W. WOLF. 1974. The cytoproct of *Paramecium caudatum*: structure and function, microtubules, and fate of food vacuole membranes. *J. Cell Sci.* **14**:611–631.
4. BATZ, W., and F. WUNDERLICH. 1976. Structural transformation of the phagosomal membrane in *Tetrahymena* cells endocytosing latex beads. *Arch. Microbiol.* **109**:215–220.
5. BOWERS, B. 1977. Comparison of pinocytosis and phagocytosis in *Acanthamoeba castellanii*. *Exp. Cell Res.* **110**:409–417.
6. BOWERS, B., and E. D. KORN. 1968. The fine structure of *Acanthamoeba castellanii*. I. The trophozoite. *J. Cell Biol.* **39**:95–111.
7. BOWERS, B., and T. E. OLSZEWSKI. 1972. Pinocytosis in *Acanthamoeba castellanii*. Kinetics and morphology. *J. Cell Biol.* **53**:681–694.
8. BOWERS, B., and T. E. OLSZEWSKI. 1974. Morphology of *Acanthamoeba* plasma membrane. Eighth International Congress on Electron Microscopy. Canberra. **2**:212–213.
9. BRANTON, D., and D. W. DEAMER. 1972. Membrane Structure. Springer-Verlag, New York.
10. DEARBORN, D., S. SMITH, and E. D. KORN. Lipophosphonoglycan of the plasma membrane of *Acanthamoeba castellanii*. Inositol and phytosphingosine content and general structural features. *J. Biol. Chem.* **251**: 2976–2982.
11. GRAHAM, R. C., and M. J. KARNOVSKY. 1966. The early stages of absorption of injected horseradish peroxidase in the proximal tubules of mouse kidney: Ultrastructural cytochemistry by a new technique. *J. Histochem. Cytochem.* **14**:291–301.
12. HEUSER, J. E., and T. S. REESE. 1973. Evidence for recycling of synaptic vesicle membrane during transmitter release at the frog neuromuscular junction. *J. Cell Biol.* **57**:315–344.
13. KITAJIMA, Y., and G. A. THOMPSON, JR. 1977. Differentiation of food vacuolar membranes during endocytosis in *Tetrahymena*. *J. Cell Biol.* **75**:436–445.
14. KLOETZEL, J. A. 1974. Feeding in ciliated protozoa I. Pharyngeal disks in *Euplotes*: A source of membrane for food vacuole formation? *J. Cell Sci.* **15**:379–401.
15. KORN, E. D. 1974. Biochemistry of endocytosis. *In* Biochemistry of Cell Walls and Membranes. C. F. Fox, editor. Butterworth (Publishers) Inc., Woburn, Mass. 1–26.
16. KORN, E. D., B. BOWERS, S. BATZRI, S. R. SIMMONS, and E. J. VICTORIA. 1974 Endocytosis and exocytosis: Role of microfilaments and involvement of phospholipids in membrane fusion. *J. Supramol. Struct.* **2**:517–528.
17. MCKANNA, J. A. 1973. Cyclic membrane flow in the ingestive-digestive system of peritrich protozoans. I. Vesicular fusion at the cytopharynx. *J. Cell Sci.* **13**:663–675.
18. MOORE, P. L., H. L. BANK, N. T. BRISSIE, and S. S. SPICER. 1978. Phagocytosis of bacteria by polymorphonuclear leukocytes. A freeze-fracture, scanning electron microscope, and thin-section investigation of membrane structure. *J. Cell Biol.* **76**:158–174.
19. OLIVER, J. M., T. E. UKENA, and R. D. BERLIN. 1974. Effects of phagocytosis and colchicine on the distribution of lectin-binding sites on cell surfaces. *Proc. Natl. Acad. Sci. U. S. A.* **71**:394–398.
20. PALADE, G. E. 1959. Functional changes in the structure of cell components. *In* Subcellular Particles. T. Hayashi, editor. The Ronald Press, New York.
21. PELLETIER, G. 1973. Secretion and uptake of peroxidase by rat adenohypophyseal cells. *J. Ultrastruct. Res.* **43**:445–459.
22. RYTER, A., and B. BOWERS. 1976. Localization of acid phosphatase in *Acanthamoeba castellanii* with light and electron microscopy during growth and after phagocytosis. *J. Ultrastruct. Res.* **57**:309–321.
23. SPIES, F., W. A. M. LINNEMANS, P. H. J. TH. VERVERGAERT, J. L. M. LEUNISSEN, and P. F. ELBERS. 1975. Encystment of *Acanthamoeba castellanii* (Neff). A combined freeze etch-thin sectioning analysis of the cell surface. *Cytobiologie.* **11**:50–64.
24. STEINMAN, R. M., S. E. BRODIE, and Z. A. COHN. 1976. Membrane flow during pinocytosis. A stereologic analysis. *J. Cell Biol.* **68**:665–687.
25. VAN ALPHEN, L., A. VERKLEIJ, J. LEUNISSEN-BIJVELT, and B. LUGTENBERG. 1978. Architecture of the outer membrane of *Escherichia coli*. III. Protein-lipopoly-saccharide complexes in intramembranous particles. *J. Bacteriol.* **134**:1089–1098.
26. VERKLEIJ, A. J., C. MOMBERS, J. LEUNISSEN-BIJVELT, and P. H. J. TH. VERVERGAERT. 1979. Lipidic intramembranous particles. *Nature (Lond.).* **279**:162–163.
27. VERKLEIJ, A. J., and P. H. J. TH. VERVERGAERT. 1975. The architecture of biological and artificial membranes as visualized by freeze-etching. *Annu. Rev. Phys. Chem.* **26**:101–122.
28. WEISMAN, R., and E. D. KORN. 1967. Phagocytosis of latex beads by *Acanthamoeba*. I. Biochemical properties. *Biochemistry.* **6**:485–497.
29. WETZEL, M. G., and E. D. KORN. 1969. Phagocytosis of latex beads by *Acanthamoeba castellanii* (Neff). III. Isolation of the phagocytic vesicles and their membranes. *J. Cell Biol.* **43**:90–104.